Published in final edited form as:
J Anal Oncol. ; 1(1): 1–9. doi:10.6000/1927-7229.2012.01.01.1.

Targeting Mantle Cell Lymphoma with Anti-SYK Nanoparticles

Ingrid Cely[1,2], **Seang Yiv**[1], **Qian Yin**[3], **Anoush Shahidzadeh**[1,2], **Li Tang**[3], **Jianjun Cheng**[3], and **Fatih M. Uckun**[1,2]

[1]Developmental Therapeutics Program, Children's Hospital Los Angeles, Children's Center for Cancer and Blood Diseases, Los Angeles, CA 90027

[2]Department of Pediatrics and Norris Comprehensive Cancer Center, University of Southern California Keck School of Medicine, Los Angeles, CA 90027

[3]Department of Materials Science and Engineering, University of Illinois at Urbana-Champaign, Urbana, Illinois 61801

Abstract

The pentapeptide mimic 1,4-bis(9-*O*-dihydroquinidinyl)phthalazine / hydroquinidine 1,4-phathalazinediyl diether ("compound 61") (C-61) is the first reported inhibitor targeting the P-site of SYK. Here we report a nanotechnology platform to target C-61 to mantle cell lymphoma (MCL) cells. Liposomal nanoparticles (NP) loaded with C-61 were prepared using the standard thin film evaporation method. The entrapment of C-61 was obtained using the pH gradient procedure with lactobionic acid (LBA) being used as a low pH buffer inside the NP. Formulation F6A was selected as a lead candidate for further biological testing. The average diameter, zeta potential and C-61 content of the F6A NP was 40 nm, 0.1 mV, and 12.6 mg/ml, respectively. F6A induces apoptosis in SYK^+ but not SYK^- leukemia/lymphoma cells. We also evaluated the cytotoxic activity of F6A in the context of an *in vitro* artificial bone marrow assay platform based on a 3D scaffold with inverted colloidal crystal geometry mimicking the structural topology of actual bone marrow matrix. The ability of C-61 to induce apoptosis in ALL-1 cells was not adversely affected by the scaffolds. F6A, but not the drug-free NP formulation F6B, caused apoptosis of MCL cell lines MAVER-1 and MINO within 24h. Further development of rationally designed SYK inhibitors and their nanoscale formulations may provide the foundation for therapeutic innovation against a broad spectrum of lymphoid malignancies, including MCL.

Introduction

Non-Hodgkin lymphoma (NHL), the most common lymphohematopoietic malignancy in the US, is a biologically heterogenous group of diseases. Mantle cell lymphoma (MCL) represents a subgroup of poor prognostic, high-risk NHL with an aggressive biology and short progression-free as well as overall survival (1-3). Therefore, identification and evaluation of active new agents and new drug combinations against MCL (4-8), including exploratory single agent Phase II clinical studies in relapsed or refractory MCL (4,9-16), as well as more intense multimodality strategies with immunochemotherapy and hematopoietic stem cell transplantation for eligible patients (17,18), have been focal points in translational lymphoma research (3). Likewise, several research teams have embarked upon molecular target discovery efforts to identify new druggable targets in MCL cells using integrated multi-platform laboratory and in silico research tools (19-22). The insights provided by translational and clinical research efforts have resulted in improvement of the overall

Corresponding Author: Fatih M. Uckun, M.D., Ph.D., Children's Hospital Los Angeles, MS#160, Los Angeles, California 90027-0367. fmuckun@chla.usc.edu; Phone: (323)-361-4328.

survival in MCL and increased the number of available salvage treatment options for patients with recurrent disease (3).

SYK is an emerging new molecular target for the treatment of B-lineage leukemias and lymphomas (23). Recent studies have established SYK as a master regulator of apoptosis controlling the activation of the PI3-K/AKT, NFκB, and STAT3 pathways, three major anti-apoptotic signaling pathways in B-lineage leukemia/lymphoma cells, including MCL cells (23). Constitutive activation and anti-apoptotic function of SYK kinase have been documented for several B-lineage lymphoid malignancies, including B-lineage ALL, chronic lymphocytic leukemia (CLL) (29-33), follicular lymphoma, diffuse large B-cell lymphoma (DLBCL) as well as MCL (23). In MCL, the *syk* gene is amplified at the DNA level, and overexpressed at both RNA and protein levels (37). Rinaldi et al. reported that low doses of the SYK inhibitor piceattanol induced cell cycle arrest and apoptosis in an MCL cell line overexpressing SYK (24). The biological significance of SYK expression in MCL cells was independently confirmed by Leseux et al. who demonstrated that SYK inhibition by piceatannol or RNAi knockdown of SYK expression using siRNA plasmids inhibits the anti-apoptotic PI3-kinase/mTOR pathway in MCL cells (25). Likewise, another SYK inhibitor, R406, was found to cause apoptosis in an MCL cell line (26). Fostamatinib disodium (R788), a prodrug of R406 in an oral formulation, showed early evidence of possible clinical activity against MCL with 1 of 9 patients achieving a PR and 4 patients showing stable disease after treatment (27).

In the present study, we explored a nanotechnology platform to target a rationally designed potent and highly selective SYK inhibitor to MCL cells. The payload of the designed liposomal nanoparticles was the pentapeptide mimic 1,4-bis(9-*O*-dihydroquinidinyl) phthalazine / hydroquinidine 1,4-phathalazinediyl diether (“compound 61”) (C-61), which is the first reported inhibitor targeting the P-site of SYK and the first apoptosis-promoting anti-cancer drug candidate in the cinchona alkaloid compound class (28, 29). A liposomal nanoparticle (NP) formulation of C-61 caused apoptotic destruction of MCL cells within 24 h. Further development of C-61 loaded NP formulations may provide the foundation for effective treatments for therapy-refractory MCL.

Materials and Methods

Materials

Dipalmitoyl phosphatidylcholine (DPPC), Cholesterol (CHOL), 1,2-distearoyl-*sn*-glycero-3-phosphoethanolamine-*N*-[methoxy(polyethylene glycol)-2000] (DSPE-PEG2000) were obtained from Avanti Polar Lipids (Alabaster, AL). LBA and sucrose were obtained from Sigma (St Louis, MO). PD-10 desalting column packed with Sephadex G-25 medium was obtained from GE Healthcare (Piscataway, NJ).

Cells

We used the following cell lines: ALL-1 (Ph^+ ALL, B-lineage, SYK^+) (29-31), REH (ALL, B-lineage, SYK^+; ATCC® CRL-8286™), MOLT-3 (T-lineage, SYK^-, ATCC® CRL-1552™), LOUCY (T-lineage, SYK^+; ATCC® CRL-2629™), MAVER-1 (Mantle cell lymphoma; SYK^+, ATCC® CRL-3008™), and MINO (Mantle cell lymphoma, SYK^+; ATCC® CRL-3000™).

Preparation of Liposomal Nanoparticles

Liposomal NPs were prepared in a round bottom flask using the standard thin film evaporation method. The entrapment of C-61 was obtained using the pH gradient procedure with Lactobionic acid (LBA) being used as a low pH buffer inside the NPs. Chloroform

used in the NP formulation was removed using a rotary evaporator at 40°C. NPs were prepared using a fixed ratio of DPPC to CHOL. Their concentrations in the NPs were kept constant. LBA solution was added to the NP film; the film was hydrated slowly with gentle hand mixing or rocking the flask at ambient temperature for about 1 hour or until all the film was dispersed to yield a milky suspension. In order to obtain a nano-sized homogeneous NP formulation, the suspension was placed in the chamber of an extruder, and extrusion was performed at 60°C, twice through 0.2-μm, then 5 times through 0.1-μm polycarbonate filters. To establish a pH gradient, the external phase of the extruded preparation was passed through a PD-10 desalting column packed with Sephadex G-25 medium, which has been pre-equilibrated with 10% sucrose. After this external phase replacement step, the pH value of the preparation solution was tuned to around 3. A weighed amount of C-61 was added to the external-phase-replaced sample. After the addition of C-61, the preparation solution was stirred at room temperature for 60 min to allow the incorporation of C-61 in the acidic interior of the liposomal NPs. For preparation of PEGylated liposome formulations, a weighed amount of DSPE-PEG2000 was added following the addition of C-61. The addition of PSPE-PEG2000 and its insertion onto the outer surface of the liposome nanoparticles were carried out at 50°C with the solution being stirred for 50 minutes. The pH of the preparation solution was adjusted to neutral through the addition of NaOH. In the final step, the NPs prepared were filtered through 0.22-μm filter and stored at 4°C in a refrigerator for the characterization of NP physical properties and for biological testing.

Physicochemical Characterization of Nanoparticles

C-61 NPs were characterized using well-established methods. Size measurement by dynamic light scattering (DLS) technique was performed on a DynaPro Titan Instrument (Wyatt Technology Corp., Santa Barbara, CA) equipped at the USC Nano BioPhysics Laboratory. Sample was loaded to a quartz cell with a sample volume of 20 μl for the DLS analysis. The particle size was obtained by averaging the data obtained of at least 10 measurements with 10 sec per acquisition. For the measurement of C-61 concentrations, NP samples were analyzed on an Agilent 1100 HPLC system equipped with a Hypersil ODS reverse phase analytical column (Hewlett Packard Hypersil 5 μm ODS, 125 × 4.6 mm) and a diode array detector with detection and reference wavelengths set at 230 nm and 420 nm, respectively. Acetonitrile: water (20:80 v/v) containing 0.1% trifluoacetic acid and 0.1% triethylamine was used as the mobile phase. The Zeta potential measurements were carried out on a Brookhaven Instrument ZetaPlus (Holtsville, NY).

Confocal Microscopy

Confocal microscopy was used as previously described (29, 30) to evaluate the structural damage of leukemia/lymphoma cells caused by C-61 NP. UltraCruz Mounting Medium containing 1.5 μg/ml of 4′,6-diamidino-2-phenylindole (DAPI) was purchased from Santa Cruz Biotechnology, Inc. (Santa Cruz, CA). The mouse monoclonal anti-Tubulin antibody was purchased from Sigma. Green-fluorescent Alexa Fluor 488 dye-labeled secondary antibody Alexa Fluor 488 goat antimouse IgG (A-11001) for confocal microscopy was purchased from Invitrogen (Carlsbad, CA). During confocal imaging, slides were imaged using the PerkinElmer Spinning Disc Confocal Microscope and the PerkinElmer UltraView ERS software (Shelton, CT).

Apoptosis Assays

Cells were treated for 24 h (37°C, 5% CO_2) with increasing concentrations of NP formulations in the absence or presence of artificial 3D cell culture scaffolds (Perfecta3DTM Cell Culture Scaffolds, 3D Biomatrix, Ann Arbor, MI). Apoptotic death was monitored using multiparameter flow cytometry, as previously reported (31). Exposure of phosphatidylserine to the outer leaflet of the target leukemia/lymphoma cell membrane was

measured using FITC-conjugated annexin V, the natural ligand of phosphatidylserine. Cells were labeled with PI and annexin V-FITC using the Annexin V-FITC apoptosis detection kit (Sigma, Catalog # APOAF-50TST) according to the manufacturer's recommendations. The labeled cells were analyzed on a LSR II flow cytometer (Becton Dickinson, Lakes, NJ).

Results

Physicochemical Characteristics of C-61 Loaded Nanoparticles (NP)

Liposomal NPs loaded with C-61 were prepared using thin film evaporation method and the entrapment of C-61 was obtained using the pH gradient procedure with lactobionic acid (LBA) being used as a low pH buffer inside the NPs as described in Materials and Methods. The concentration of LBA alone had a profound effect on C-61 entrapment. Within the concentration range of 100-400 mM LBA, the C-61 content increased nearly linearly with the LBA concentration. A level of 12.6 mg/ml of C-61 has been reached in NP formulations F5A and F6A (400 mM LBA formulations). This represented a 6-fold increase from the 2.1 mg/ml of C-61 in NP formulation F1A (100 mM LBA). Formulation F6A was selected as the lead candidate for further biological testing. The average diameter of the F6A NP was 38 nm with a zeta potential of 0.1 mV and C-61 content of ~12.6 mg/ml (Table 1)

Pro-apoptotic Activity of C-61 NP Formulation F6A Against SYK-Expressing Leukemia and Lymphoma Cells

We first examined the selectivity and cytotoxicity of C-61 NP formulation F6A against SYK^+ vs. SYK^- leukemia/lymphoma cells. F6A, (but not the drug-free NP formulation F6B), caused apoptotic destruction of SYK-expressing LOUCY cells (Figure 1A) but it was not cytotoxic to SYK-negative MOLT-3 cells (Figure 1B). We also examined the ability of C-61 NP to induce apoptosis in radiochemotherapy-resistant B-lineage acute lymphoblstic leukemia (ALL) cell lines ALL-1 (Ph^+) and REH. Within 24h of exposure, F6A caused apoptosis in both cell lines in a concentration-dependent fashion (Figure 2), while F6B did not induce apoptosis. We also evaluated the cytotoxic activity of F6A in the context of Perfecta3D™ Cell Culture Scaffolds, an *in vitro* artificial bone marrow assay platform based on a 3D scaffold with inverted colloidal crystal (ICC) geometry mimicking the structural topology of actual bone marrow matrix (32). The ability of F6A to induce apoptosis in ALL-1 cells was not adversely affected by the scaffolds (Figure 3).

C-61 Loaded NP Formulation F6A Directs Mantle Cell Lymphoma (MCL) Cells to Self-Destruct

We next examined the ability of C-61 loaded NP F6A to induce apoptosis in MCL cell lines. By using a quantitative flow cytometric apoptosis assay, we documented that within 24 hours of treatment with 0.1-10 μg/mL F6A (but not the drug free F6B control) apoptosis is induced in a concentration-dependent fashion. At ≥3 μg/mL, less than 20% of MAVER-1 cells remained viable, which represents a marked reduction from the 85.7% viability of untreated control cells and the percentage of cells with advanced apoptosis ranged from 18% at 3 μg/mL (at this concentration 67% of the cells were in early apoptosis) to 74% at 10 μg/mL F6A (Figure 4). In contrast, 84.7% of MAVER-1 cells treated with drug-free NPs included as a vehicle control remained viable with no signs of apoptosis. Similar results were obtained in a separate experiment in which 10 μg/ml F6A caused apoptosis in 99.6% of MAVER-1 cells and reduced the percentage of viable MAVER cells from 84.8% at baseline to 0.3% (Figure 5A). In contrast, 86.5% of MAVER-1 cells treated with F6B remained viable. Similar to MAVER-1 cells, MINO cells were also rapidly killed by F6A (Figure 5B).

Discussion

The efficient delivery of the various SYK inhibitors by leveraging nanotechnology holds particular promise for treatment of leukemias and lymphomas, including MCL. Liposomal NP therapeutics containing active anti-cancer agents may provide the foundation for potentially more effective and less toxic anti-cancer treatment strategies due to their improved pharmacokinetics, reduced systemic toxicity, and increased intra-tumoral/intra-cellular delivery (33-35). NPs have been coated with polyethylene glycol (PEG) (i.e., PEGylated) in an attempt to render their resistant against protein adsorption, enhance their biocompatibility, and stabilize them against agglomeration in biological environments. PEGylated NPs with diameter around 100-nm may become long-circulating in the blood stream and have been called stealth particles since they can evade recognition by T-cells and macrophages, and avoid rapid clearance by the immune system (33, 34). NPs that are sterically stabilized by PEG polymers on their surface and have surface charges that are slightly negative or slightly positive have minimal self-self or self-non-self interactions and improved pharmacokinetics. PEGylation of NP creates a hydrophilic surface and leads to increased protein solubility, reduced immunogenicity, prolonged plasma half life due to prevention of rapid renal clearance, and reduced clearance by the reticuloendothelial system (RES) system due to decreased macrophage capture and opsonization (33, 34). Rationally engineered NP constructs of SYK inhibitors are likely to be less toxic and more effective than free molecules.

NPs can be functionalized with a tumor targeting moiety such as a ligand or engineered antibody fragments directed against a surface receptor on cancer cells in order to achieve optimal tumor targeting and site-specific drug delivery to further reduce their toxicity and improve their efficacy (33-35). When linked with tumor targeting moieties, NPs can bind the cancer cells that have overexpressed receptors with high affinity and precision. The targeting ligands enable NPs to bind to cell surface receptors and enter cells by receptor-mediated endocytosis. In our own program, efforts are underway to prepare NPs targeted against surface receptors on MCL cells. Further development of rationally designed SYK inhibitors and their nanoscale formulations may provide the foundation for therapeutic innovation against a broad spectrum of lymphoid malignancies, including MCL.

Acknowledgments

The project described was supported in part by DHHS grants P30CA014089, U01-CA-151837, and R01CA-154471 (FMU) from the National Cancer Institute and the NIH Director’s New Innovator Award 1DP2OD007246 (JC). The content is solely the responsibility of the authors and does not necessarily represent the official views of the National Cancer Institute or the National Institutes of Health. This work was also supported in part by Children’s Hospital Los Angeles Institutional Endowment and Special Funds, 2011 V-Foundation Translational Research Award, Ronald McDonald House Charities of Southern California, Couples Against Leukemia Foundation and a William Lawrence & Blanche Hughes Foundation grant. We further thank all members of the Uckun lab for their many invaluable technical assistance and contributions. We also thank Dr. Nickolas Chelyapov of the USC NanoBiophysics Core Facility and Ernesto Barron of the USC Norris Comprehensive Cancer Center Cell and Tissue Imaging Core for their assistance.

References

1. Witzig TE. Current treatment approaches for mantle-cell lymphoma. J Clin Oncol. 2005; 23:6409–6414. [PubMed: 16155027]
2. Brody J, Advani R. Treatment of mantle cell lymphoma: Current approach and future directions. Crtical Reviews in Oncology/Hematology. 2006; 58:257–265.
3. Williams ME, Connors JM, Dreyling MH, Gascoyne RD, Kahl BS, Leonard JP, Press OW, Wilson WH. Review. Mantle cell lymphoma: report of the 2010 Mantle Cell Lymphoma Consortium Workshop. Leukemia & lymphoma. 2011; 52:24–33. [PubMed: 21133727]

4. Delmonte A, Ghielmini M, Sessa C. Beyond monoclonal antibodies: New therapeutic agents in non-Hodgkin's lymphomas. The Oncologist. 2009; 14:511–525. [PubMed: 19411316]
5. Samad N, Younes A. Temsirolimus in the treatment of relapsed or refractory mantle cell lymphoma. Onco Targets Ther. 2010; 3:167–78. [PubMed: 20856791]
6. Qi W, Cooke LS, Liu X, Rimsza L, Roe DJ, Manziolli A, Persky DO, Miller TP, Mahadevan D. Aurora inhibitor MLN8237 in combination with docetaxel enhances apoptosis and anti-tumor activity in mantle cell lymphoma. Biochemical Pharmacology. Febr;2011 DOI 10.1016/j.bcp.2011.01.017. Epub ahead of print.
7. Singh AT, Evens AM, Anderson RJ, Beckstead JA, Sankar N, Sassano A, Bhalla S, Yang S, Platanias LC, Forte TM, Ryan RO, Gordon LI. All trans retinoic acid nanodisks enhance retinoic acid receptor mediated apoptosis and cell cycle arrest in mantle cell lymphoma. Br J Hematol. 2010; 150:158–69.
8. Romaguera JE, Fayad LE, McLaughlin P, Pro B, Rodriguez A, Wang M, Weaver P, Hartig K, Kwak LW, Feldman T, Smith J, Ford P, Goldberg S, Pecora A, Goy A. Phase I trial of bortezomib in combination with rituximab-HyperCVAD alternating with rituximan, methotrexate and cytarabine for untreated aggressive mantle cell lymphoma. Br J Hematol. 2010; 151:47–53.
9. O'Connor OA, Portlock C, Moskowitz C, Struas D, Hamlin P, Stubblefield M, Dumetrescu O, Colevas AD, Grant B, Zelenetz A. A multicentre phase II clinical experience with the novel azaepotholone Ixabepilone (BMS247550) in patients with relapsed or refractory indolent non-Hodgkin lymphoma and mantle cell lymphoma. Br J Hematol. 2008; 143:201–9.
10. O'Connor OA, Moskowitz C, Portlock C, Hamlin P, Straus D, Dumitrescu O, Sarasohn D, Gonen M, Butos J, Neylon E, Hamelers R, Cortelli BM-G, Blumel S, Zelenetz AD, Gordon L, Wright JJ, Vose J, Cooper B, Winter J. Patients with chemotherapy-refractory mantle cell lymphoma experience high response rates and identical progression-free survivals compared with patients with relapsed disease following treatment with single agent bortezomib: results of a multicentre phase 2 clinical trial. Br J Hematol. 2009; 145:34–39.
11. Yee KW, Zeng Z, Konopleva M, Verstovsek S, Ravandi F, Ferrajoli A, Thomas D, Wierda W, Apostolidou E, Albitar M, O'Brien S, Andreef M, Giles FJ. Phase I/II study of the mammalian target of rapamycin inhibitor everolimus (RAD001) in patients with relapsed or refractory hematologic malignancies. Clin Cancer Res. 2006; 12:5165–73. [PubMed: 16951235]
12. Morschhauser F, Depil S, Jourdan E, Wetterwald M, Bouabdalah R, Marit G, Solal-Celigny P, Sebban C, Coiffier B, Chouaki N, Bauters F, Dumontet C. Phase II study of gemcitabine-dexamethasone with or without cisplatin in relapsed or refractory mantle cell lymphoma. Annals of Oncology. 2007; 18:370–375. [PubMed: 17074972]
13. Witzig TE, Vose JM, Zinzani L, Reeder CB, Buckstein R, Polikoff JA, Bouabdallah R, Haioun C, Tilly H, Guo P, Pietronigro D, Ervin-Haynes AL, Czuczman MS. An international phase II trial of single-agent lenalidomide for relapsed or refractory aggressive B-cell non-Hodgkin's lymphoma. Annals of Oncology. Jan 12.2011 advance access published.
14. Witzig TE, Reeder CB, LaPlant BR, Gupta M, Johnston PB, Micallef IN, Porrata LF, Ansell SM, Colgan JP, Jacobsen ED, Ghobrial IM, Habermann TM. A phase II trial of the oral mTOR inhibitor everolimus in relapsed aggressive lymphoma. Leukemia. 2011; 25:341–347. [PubMed: 21135857]
15. Friedberg JW, Vose JM, Kelly JL, Young F, Bernstein SH, Peterson D, Rich L, Blumel S, Proia NK, Liesveld J, Fisher RI, Armitage JO, Grant S, Leonard JP. The combination of bendamustine, bortezomib and rituximab for patients with relapsed/refractory indolent and mantle cell non-Hodgkin lymphoma. Blood. Jan 14.2011 prepublished online. DOI 10.1182/blood-2010-11-314708.
16. Wang M, Oki Y, Pro B, Romaguera JE, Rodriguez MA, Samaniego F, McLaughlin P, Hagemeister F, Neelapu S, Copeland A, Samuels BI, Loyer EM, Ji Y, Younes A. Phase II study of Tttrium-90-Ibritumomab Tiuxetan in patients with relapsed or refractory mantle cell lymphoma. J Clin Oncol. 2009; 27:5213–5218. [PubMed: 19770379]
17. Jacobsen E, Freedman A. An update on the role of high-dose therapy with autologous or allogeneic stem cell transplantation in mantle cell lymphoma. Curr Opin Oncol. 2004; 16:106–13. [PubMed: 15075900]

18. Damon LE, Johnson JL, Niedzwiecki D, Cheson BD, Hurd DD, Bartlett NL, LaCasce AS, Blum KA, Byrd JC, Kelly M, Stock W, Linker CA, Canellos GP. Immunochemotherapy and autologous ste—cell transplantation for untreated patients with mantle-cell lymphoma: CALGB 59909. J Clin Oncol. 2009; 27:6101–6108. [PubMed: 19917845]

19. Greiner TC, Dasgupta C, Ho VV, Weisenburger DD, Smith LM, Lynch JC, Vose JM, Fu K, Armitage JO, Braziel RM, Campo E, Delabie J, Gascoyne RD, Jaffe ES, Muller-Hermelink HK, Ott G, Rosenwald A, Staudt LM, Im MY, Karaman MW, Pike BL, Chan WC, Hacia JG. Mutation and genomic deletion status of ataxia telangiectasia mutated (ATM) and p53 confer specific gene expression profiles in mantle cell lymphoma. Proc. Natl Acad Sci USA. 2006; 103:2352–7. [PubMed: 16461462]

20. Psyrri A, Papageorgiu S, Liakata E, Scorilas A, Rontogianni D, Kontos CK, Argyriou P, Pectasides D, Harhalakis N, Pappa V, Koliatexi A, Economopoulou C, Kontsioto F, Maratou E, Economopoulos T. Phosphatidylinositol 3′-Kinase catalytic subunit a gene amplification contributes to the pathogenesis of mantle cell lymphoma. Clin Cancer Res. 2009; 15:5724–32. [PubMed: 19723646]

21. Hartmann EM, Campo E, Wright G, Lenz G, Salaverria I, Jares P, Xiao W, Braziel RM, Rimsza LM, Chan W-C, Weisenburger DD, Delabie J, Jaffe ES, Gascoyne RD, Dave SS, Mueller-Hermelink H-K, Staudt LM, Ott G, Bea S, Rosenwald A. Pathway discovery in mantle cell lymphoma by integrated analysis of high-resolution gene expression and copy number profiling. Blood. 2010; 116:953–961. [PubMed: 20421449]

22. Leschchenko VV, Kuo P-Y, Shaknovich R, Yang DT, Gellen T, Petrich A, Yu Y, Remache Y, Weniger MA, Rafiq S, Suh S, Goy A, Wilson W, Verma A, Braunschweig I, Muthusamy N, Kahl BS, Byrd JC, Wiestner A, Melnick A, Parekh S. Genomewide DNA methylation analysis reveals novel targets for drug development in mantle cell lymphoma. Blood. 2010; 116:1025–1034. [PubMed: 20427703]

23. Uckun FM, Qazi S. Spleen tyrosine kinase as a molecular target for treatment of leukemias and lymphomas. Expert Rev Anticancer Ther. 2010; 10(9):1407–18. [PubMed: 20836676]

24. Rinaldi A, Kwee I, Taborelli M, Largo C, Uccella S, Martin V, Poretti G, Gaidano G, Calabrese G, Martinelli G, Baldini L, Pruneri G, Capella C, Zucca E, Cotter FE, Ciqudosa JC, Catapano CV, Tibiletti MG, Bertoni F. Genomic and expression profiling identifies the B cell associated tyrosine kinase Syk as a possible therapeutic target in mantle cell lymphoma. Br J Hematol. 2006; 132:303–16.

25. Leseux L, Hamdi SM, Al Saati T, Capilla F, Recher C, Laurent G, Bezombes C. Syk-dependent mTOR activation in follicular lymphoma cells. Blood. 2006; 108(13):4156–62. [PubMed: 16912221]

26. Tauzin S, Ding H, Burdevet D, Borisch B, Hoessli DC. Membrane-associated signaling in human B-lymphoma lines. Exp Cell Res. 2011; 317(2):151–62. [PubMed: 20875408]

27. Friedberg JW, Sharman J, Sweetenham J, Johnston PB, Vose JM, Lacasce A, Schaefer-Cutillo J, De Vos S, Sinha R, Leonard JP, Cripe LD, Gregory SA, Sterba MP, Lowe AM, Levy R, Shipp MA. Inhibition of Syk with fostamatinib disodium has significant clinical activity in non-Hodgkin lymphoma and chronic lymphocytic leukemia. Blood. 2010; 115(13):2578–85. [PubMed: 19965662]

28. Uckun FM, Qazi S, Ma H, Tuel-Ahlgren L, Ozer Z. STAT3 is a substrate of SYK tyrosine kinase in B-lineage leukemia/lymphoma cells exposed to oxidative stress. Proc. Natl. Acad. Sci. USA. 2010; 107(7):2902–7. [PubMed: 20133729]

29. Uckun FM, Ek RO, Jan ST, Chen CL, Qazi S. Targeting SYK Kinase-Dependent Anti-Apoptotic Resistance Pathway in B-lineage Acute Lymphoblastic Leukemia (ALL) Cells with a Potent SYK Inhibitory Pentapeptide Mimic. British Journal of Haematology. 2010; 149(4):508–17. [PubMed: 20151979]

30. Uckun FM, Goodman P, Ma H, Dibirdik I, Qazi S. CD22 Exon 12 Deletion as a Novel Pathogenic Mechanism of Human B-Precursor Leukemia. Proc. Natl. Acad. Sci. USA. 2010; 107:16852–16857. [PubMed: 20841423]

31. Uckun FM, Qazi S, Ozer Z, Garner AL, Pitt J, Ma H, Janda KD. Inducing apoptosis in chemotherapy-resistant B-lineage acute lymphoblastic leukemia (ALL) cells by targeting GRP78/

HSPA5, a master regulator of the anti-apoptotic unfolded protein response (UPR) signaling network. British Journal of Haematology. 2011 in press (MS# BJH-2011-00084).

32. Nichols JE, Cortiella J, Lee J, Niles JA, Cuddihy M, Wang S, Bielitzki J, Cantu A, Mlcak R, Valdivia E, Yancy R, McClure ML, Kotov NA. In vitro analog of human bone marrow from 3D scaffolds with biomimetic inverted colloidal crystal geometry. Biomaterials. Feb; 2009 30(6): 1071–9. [PubMed: 19042018]
33. Davis ME, Chen Z, Shin DM. Nanoparticle therapeutics: an emerging treatment modality for cancer. Nature Review Drug Discovery. 2008; 7:771–82.
34. Cho K, Wang X, Nie S, Chen ZG, Shin DM. Therapeutic nanoparticles for drug delivery in cancer. Clin Cancer Res. Mar 1; 2008 14(5):1310–6. [PubMed: 18316549]
35. Cheng WW, Allen TM. The use of single chain Fv as targeting agents for immunoliposomes: an update on immunoliposomal drugs for cancer treatment. Expert Opin. Drug Deliv. 2010; 7:461–478. [PubMed: 20331354]

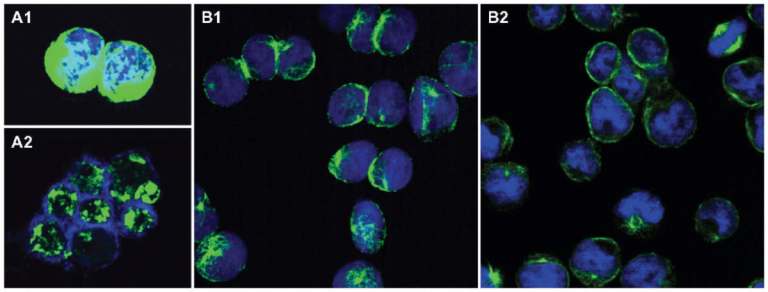

Figure 1. PEGylated C-61 Nanoparticle Formulation F6A Induced Apoptosis in SYK^{+} (but not SYK^{-}) Human T-lineage Leukemia/Lymphoma Cells

[A] Confocal images of SYK-expressing LOUCY cells treated for 24 h with drug-free control formulation F6B (Panel A.1) vs. 1 μg/mL C-61 loaded formulation F6A (Panel A.2) showing nuclear (Blue) destruction and loss of tubulin (Green) cytoskeleton. [B] Confocal images of SYK-negative MOLT-3 cells treated for 24 h with drug-free control formulation F6B (Panel B.1) vs. 1 μg/mL C-61 loaded formulation F6A (Panel B.2) showing no evidence of cell damage.

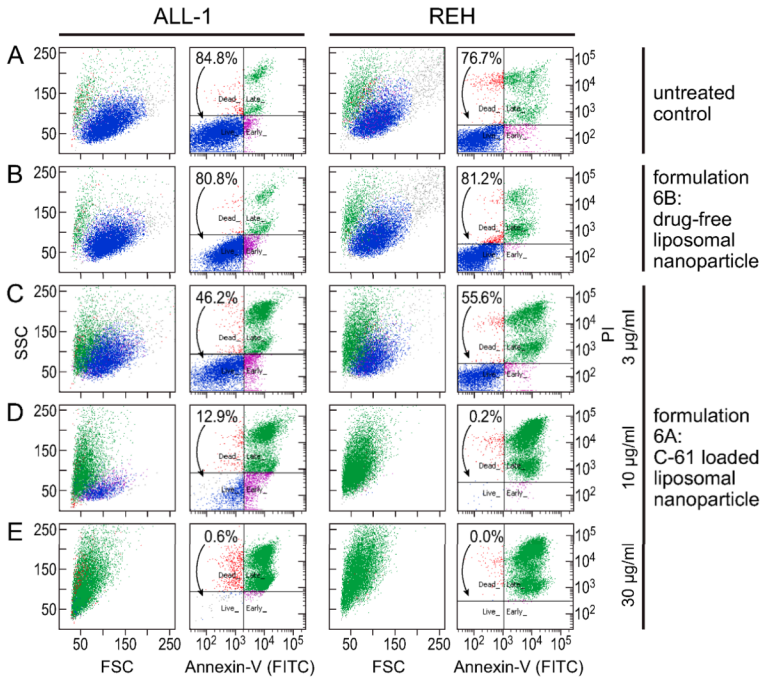

Figure 2. C-61 Nanoparticle Formulation F6A Induces Apoptosis in ALL Cell Lines ALL-1 [A] and REH [B]

Representative FACS histograms of ALL-1 and REH cells treated with Formulation F6A vs. Formulation F6B. Cells were treated for 24h at 37°C with 3-30 μg/mL Formulation F6A, an equal volume of C-61 free Formulation F6B corresponding to the volume of F6A at the highest concentration or left untreated. Cells were analyzed for apoptosis using the standard quantitative flow cytometric apoptosis assay using the Annexin V-FITC Apoptosis Detection Kit from Sigma. Whereas drug-free NP formulation F6B was not cytotoxic, Formulation F6A caused apoptosis in the majority of the treated ALL cells. The anti-leukemic potency of C-61 nanoparticle formulation F6A is evidenced by the significantly lower percentages of Annexin V-FITC^{-}PI^{-} live cells located in the left lower quadrant of the corresponding two-color FACS histogram as well as substantially higher percentage of apoptotic cells (in green) with marked shrinkage and altered SSC in the corresponding FSC/SSC light scatter plot.

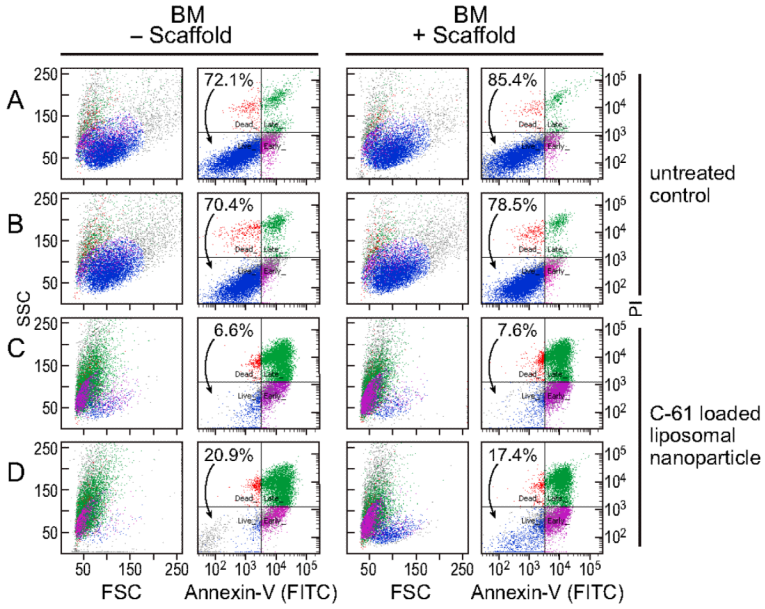

Figure 3. C-61 NP Formulation F6A Induces Apoptosis in ALL Cells in the Presence or Absence of 3D Tissue Culture Scaffolds

ALL-1 were treated in duplicate with C-61 loaded NP formulation F6A (~14 μM) for 24 hrs at 37°C in the absence (A) or presence (B) of artificial 3D cell culture scaffolds (Perfecta3D™ Cell Culture Scaffolds, 3D Biomatrix, Ann Arbor, MI). Cells were analyzed for apoptosis using the standard quantitative flow cytometric apoptosis assay using the Annexin V-FITC Apoptosis Detection Kit from Sigma. F6A induced apoptosis in ALL-1 cells within 24 h. The potency of C-61 NP is evidenced by the significantly reduced percentage of Annexin V-FITC^{-} PI^{-} live cells located in the left lower quadrant of the corresponding two-color FACS histogram as well as substantially higher percentage of apoptotic cells (in green) with marked shrinkage and altered SSC in the corresponding FSC/SSC light scatter plot.

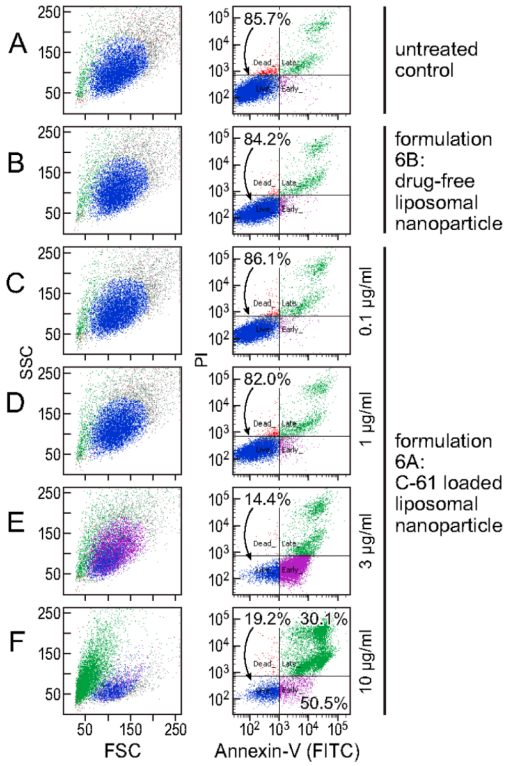

Figure 4. C-61 NP Induce Apoptosis in Mantle Cell Lymphoma Cell Line MAVER-1

Representative FACS histograms (obtained using a BD LSR-II flow cytometer) of MAVER cells treated with drug-free NP vs. C-61 loaded NP. Cells were assayed for apoptosis using the standard quantitative flow cytometric apoptosis assay using the Annexin V-FITC Apoptosis Detection Kit from Sigma. Freshly prepared C-61 NP caused apoptosis in MAVER-1 cells in a concentration-dependent fashion. Substantially fewer MAVER-1 cells remained alive after the treatment with C-61 NP. The potency of the C-61 NP is evidenced by the significantly lower percentages of Annexin V-FITC^{-}PI^{-} live cells located in the left lower quadrant of the corresponding two-color FACS histogram as well as substantially higher percentage of apoptotic cells (in green) with marked shrinkage and abnormal SSC in the corresponding FSC/SSC light scatter plot.

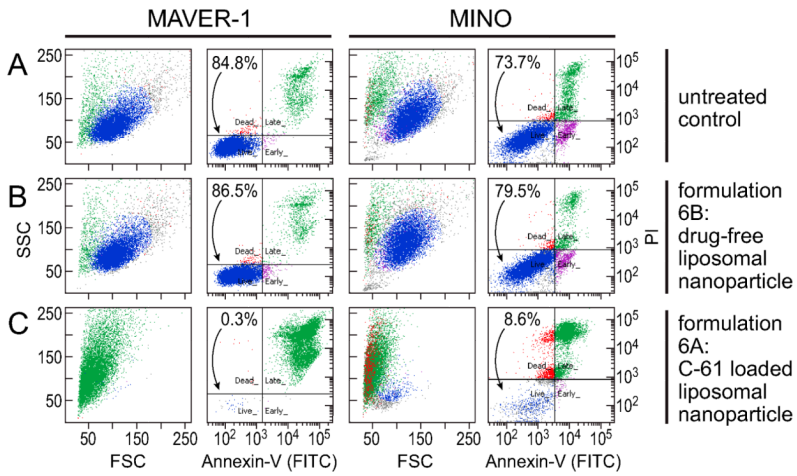

Figure 5. C-61 Nanoparticle Formulation F6A Induces Apoptosis in Mantle Cell Lymphoma (MCL) Cell Lines MAVER-1 [A] and MINO [B]

Representative FACS histograms of MAVER-1 and MINO cells treated with F6A vs. F6B. Cells were treated for 24 h at 37°C with 10.7 μg/mL (equivalent to 13.7 μM) of F6A or the same amount of F6B. Control cells were untreated. Cells were analyzed for apoptosis using the standard quantitative flow cytometric apoptosis assay using the Annexin V-FITC Apoptosis Detection Kit from Sigma. Whereas drug-free NP formulation F6B was not cytotoxic, Formulation F6A induced apoptosis in most of the treated MCL cells. The anti-MCL potency of C-61 NP formulation F6A is evidenced by the significantly lower percentages of Annexin V^{-}FITC-PI^{-} live cells located in the left lower quadrant of the corresponding two-color FACS histogram as well as substantially higher percentage of apoptotic cells (in green) with marked shrinkage and altered SSC in the corresponding FSC/SSC light scatter plot.

Table 1

C-61 Liposomal Nanoparticle Formulations

ID	DPPC	CHOL	PEG2000-DSPE	LBA	Mean Diameter	C-61 Conc.	ZP
	mg/ml	mg/ml	mg/ml	mM	nm	mg/ml	mV
001A	30	15.8	0.0	100	122	2.06	-
002A	30	15.8	0.0	200	131	4.25	-
003A	25	12.5	4.7	200	203	5.95±0.00	-
004A	30	15.8	0.0	300	174	3.80±0.04	−2.2
005A	30	15.8	0.0	400	39.8	12.61±0,17	+0.8
006A	30	15.8	3.0	400	37.8	12.63±0.15	+0.1